PROCEEDINGS, 48th Workshop on Geothermal Reservoir Engineering
Stanford University, Stanford, California, February 6-8, 2023
SGP-TR-224

Tabulated Database of Closed-Loop Geothermal Systems Performance for Cloud-Based Technical and Economic Modeling of Heat Production and Electricity Generation

Koenraad Beckers,[1] Yaroslav Vasyliv,[2] Gabriela A. Bran-Anleu,[2] Mario Martinez,[2] Chad Augustine,[1] Mark White,[3] and the Closed-Loop Geothermal Working Group

[1] *National Renewable Energy Laboratory, Golden, Colorado, USA*

[2] *Sandia National Laboratories, Albuquerque, New Mexico, USA*

[3] *Pacific Northwest National Laboratory, Richland, Washington, USA*

Keywords: closed-loop geothermal, hot-dry rock, LCOE, LCOH, u-tube, co-axial, sCO_2, techno-economic analysis, tabulated database

ABSTRACT

To better understand the heat production, electricity generation performance, and economic viability of closed-loop geothermal systems in hot-dry rock, the Closed-Loop Geothermal Working Group—a consortium of several national labs and academic institutions—has tabulated time-dependent numerical solutions and levelized cost results of two popular closed-loop heat exchanger designs (u-tube and co-axial). The heat exchanger designs were evaluated for two working fluids (water and supercritical CO_2) while varying seven continuous independent parameters of interest (mass flow rate, vertical depth, horizontal extent, borehole diameter, formation gradient, formation conductivity, and injection temperature). The corresponding numerical solutions (approximately 1.2 million per heat exchanger design) are stored as multi-dimensional HDF5 datasets and can be queried at off-grid points using multi-dimensional linear interpolation. A Python script was developed to query this database and estimate time-dependent electricity generation using an organic Rankine cycle (for water) or direct turbine expansion cycle (for CO_2) and perform a cost assessment. This document aims to give an overview of the HDF5 database file and highlights how to read, visualize, and query quantities of interest (e.g., levelized cost of electricity, levelized cost of heat) using the accompanying Python scripts. Details regarding the capital, operation, and maintenance and levelized cost calculation using the techno-economic analysis script are provided.

1. INTRODUCTION

Closed-loop geothermal systems, sometimes referred to as advanced geothermal systems, rely on a fluid circulating in a closed-loop configuration through a downhole completion to extract heat from the subsurface rocks. The fluid considered is typically water (potentially with additives) or supercritical CO_2, and does not penetrate the reservoir but stays within the wellbore. Two common designs are a U-loop configuration and a co-axial configuration (Figure 1). In a U-loop design, one or multiple laterals connect an injection well to a production well, whereas in a co-axial design, insulated tubing is installed within a wellbore and the fluid is injected either in the annulus or center pipe and produced from the other. Other designs exist, including hybrid configurations where the closed-loop system is combined with flow through fractures. While closed-loop geothermal has been proposed and studied for several decades, it recently has received significant attention and investment. Proponents highlight its potential to develop geothermal anywhere without requiring the presence of natural permeability or creation of fluid flow pathways through fractured rocks (e.g., with hydraulic stimulation to create enhanced geothermal systems [EGS] (DOE, 2022). Closed-loop technology can also be used in permeable reservoirs, for example, to repurpose idle or abandoned wells, or to deal with aggressive in situ fluid chemistry. On the other hand, constraining fluid to the wellbore limits the area for heat transfer between the rock and the fluid. For conduction-dominated systems, a low heat transfer area combined with a low rock thermal conductivity hinders efficient heat production and requires long wellbores (i.e., tens of kilometers) to obtain multi-MWe systems. Long downhole completions can become complex and costly and may require significant cost reductions from current baseline drilling costs to obtain attractive levelized cost of energy. One approach being developed by industry is drilling long open-hole laterals to reduce total drilling time and avoid casing and cement.

Various tools and simulators have been developed to study performance and cost-competitiveness of closed-loop geothermal systems. Beckers et al. (2016) developed the slender-body theory (SBT) tool for computationally efficient heat transfer simulations of various closed-loop designs in conduction-only reservoirs. Combined with models in COMSOL and the GEOPHIRES simulator (Beckers and McCabe, 2019), Beckers et al. (2022) simulated thermal and electricity output and levelized cost of energy for various closed-loop designs. Results were reported for 40 cases exploring impact of different parameters including depth, rock temperature, flow rate, injection temperature, and total borehole length. A general observation was that conduction-only reservoir systems with total borehole length of only a few kilometers are limited to electricity output in the range of tens to hundreds of kW_e, even with rock temperatures of 500°C. For all cases studied, utilizing the heat for direct utilization instead of electricity production avoids relatively low heat-to-power conversion efficiencies, translating to lower levelized costs of energy. Beckers and Johnston (2022) combined these tools with power plant models for organic Rankine cycles in IPSEpro (SimTech, 2021) and studied performance of an Eavor Loop 2.0 design. They found obtaining a levelized cost of electricity of ~$70/MWh requires a geothermal gradient of 60°C/km, a discount rate below 9%, and lateral drilling cost below $400/m, for a system with 12 lateral passes (each about 6.5 km long) with maximum vertical depth of 7.5 km depth. Horne (2022) developed a web-based tool for a U-loop design based on Ramey's wellbore heat transmission model. The tool allows for user-friendly evaluation of thermal output but does not simulate electricity production and does not estimate the cost. Other closed-loop geothermal modeling tools and studies are found in literature, including the works by Oldenburg et al. (2016) and Malek et al. (2021).

Given the recent considerable interest and investment in closed-loop geothermal, careful evaluation of performance and cost of a proposed design is recommended. Most of the tools listed above and found in literature are either not publicly accessible, do not consider economics, or require knowledge of coding (e.g., Python or MATLAB) to run the tool. In this work, we created an open-source and easy to use online tool for quick and accurate evaluation of performance and cost of closed-loop systems. The tool runs in the cloud and only requires a web browser for the user to access it, avoiding the need to configure a software environment to run the code on the user's computer. We considered both a U-loop and co-axial design, both water and sCO_2 as circulating fluid, and a range in flow rate, injection temperature, depth, lateral length, wellbore diameter, and rock thermal conductivity. Thermal performance was pre-calculated and stored in an HDF5 dataset. An online script was developed to access the dataset, estimate electricity generated, and evaluate capital, operation and maintenance, and levelized cost of heat or electricity. Our approach is presented in Section 2, including a discussion of the modeling tools, use of high-performance computing capabilities and model validation test runs. The dataset storing the subsurface simulation results, accompanying scripts and the independent and fixed parameters are discussed in Section 3. Techno-economic modeling approach, accompanying scripts and examples are discussed in Section 4. Conclusions are listed in Section 5.

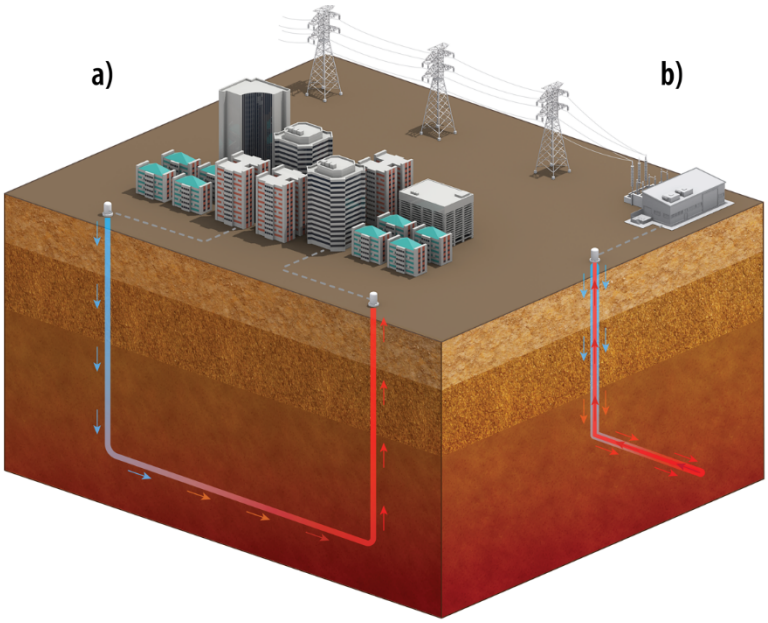

Figure 1: Two common types of closed-loop geothermal systems are: a) U-loop design (with one or multiple laterals) and b) co-axial design or "pipe-in-pipe" configuration. Photo credit: NREL.

2. APPROACH

A team composed of multiple national laboratories (i.e., Closed-Loop Geothermal Working Group) was assembled to develop a fast and user-friendly techno-economic analysis (TEA) tool for evaluating performance of closed-loop geothermal systems. In developing this tool, Sandia National Laboratories (Sandia) tabulated subsurface simulations providing estimates of production temperature, pressures, and heat for a wide range of configuration and operation conditions, National Renewable Energy Laboratory (NREL) combined the subsurface results with power plant and economic models as implemented in GEOPHIRES to estimate net electricity generation and costs, and Pacific Northwest National Laboratory was responsible for overall project management. To lower the entry barrier for users, the TEA tool, accompanying Python scripts, and HDF5 dataset have been uploaded to the cloud, allowing users to run their own TEAs in the cloud without needing to configure a Python environment on their computers.

2.1 Methodology

Previously, Vasyliv et al. (2021) developed simplified numerical models for modeling closed-loop heat exchangers using Sandia's Sierra multi-physics software suite, specifically the Aria thermal-fluids finite element package (Sierra Thermal Fluids Development Team, 2021). Comparisons to Morita et al.'s 1992 experiments (Morita et al., 1992a, 1992b) demonstrated that a 1D area averaged fluid model coupled through convective flux boundary conditions to a 2D axisymmetric transient heat conduction domain was sufficient to model the outlet state with water as a working fluid (Vasyliv et al., 2021; White et al., 2021). However, this model was insufficient for modeling fluids with strong pressure dependence (e.g., sCO_2) due to the de-coupled pressure calculation. Here, the model has been extended by coupling the time-dependent fluid thermal energy equation (temperature formulation) with the 1D steady momentum equation, thereby permitting to include an unknown fluid pressure. The 1D steady momentum equation includes inertial, pressure, viscous, and gravitational forces, where the viscous term is modeled using the Darcy-Weisbach friction factor (i.e., non-dimensional wall-shear stress) as determined

from the explicit Haaland fitting. Additional volumetric terms have been added to the thermal energy equation to account for changes in the specific internal energy accompanying thermal expansion as well as irreversible heating due to viscous dissipation.

The former term $\beta T \frac{DP}{Dt}$ is needed to accurately model sCO_2, where $\beta(T, P)$ is the isobaric expansion coefficient and where $\frac{DP}{Dt}$ is the material derivative of pressure, whereas the latter term is $0.5\,\rho u^3\, f / D_h$, where ρ is the fluid density, u is the fluid speed, D_h is the hydraulic diameter, and f is the friction factor.

The viscous dissipation term is negligible for most cases, but we have found not including it can result in a slight underprediction in the outlet temperature when compared to the SBT model. As before, material properties are evaluated using CoolProps library (Bell et al., 2014); however, now the material properties are tabulated as functions of both temperature and pressure. The resulting set of nonlinear system of equations is solved using Newton's method with preconditioned GMRES iterations for the inner linear solve.

Several validation test cases were compared against the SBT model for both water and sCO_2 as well as for both heat exchanger designs. Below in Figure 3 we highlight results for Case 11 reported in Beckers et al. 2022. For this case, sCO_2 is injected down the annulus of a coaxial heat exchanger at 20 kg/s, 40°C, and 100 bar, with a 2 km bottom borehole temperature of 200°C. Here, we've modified the case to include a 6 km lateral extension. As can be seen, the numerical solutions of both models show excellent agreement with each other, with the outlet temperatures indistinguishable from each other. Other cases investigated showed similar agreement.

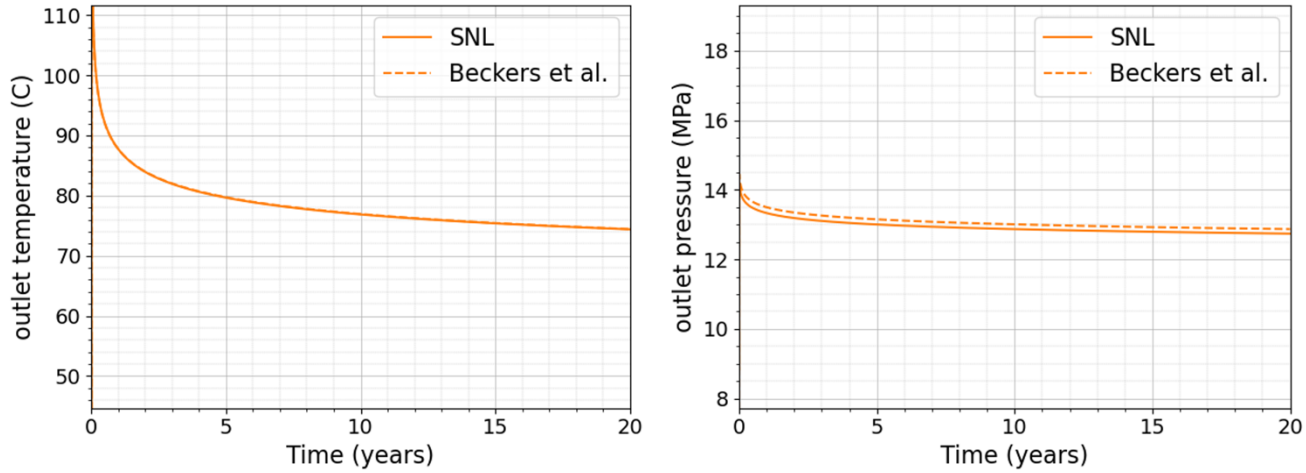

Figure 2: Outlet temperature (left) and outlet pressure (right) for a coaxial heat exchanger with sCO_2 fluid flowing down the annulus. The Sandia model ("SNL," solid line) and the SBT model (dotted line) show excellent agreement. These results correspond to a 6 km lateral extension of Case 11 as detailed in Beckers et al. (2022).

As these numerical models are cheap to solve, it is possible to directly tabulate solutions of a significant portion of the hot-dry rock design space using structured cartesian grids. While this approach suffers from the curse of dimensionality, it's favored here due to its simplicity. The design space considered corresponds to two subsurface heat exchanger designs (u-tube and co-axial), two closed-loop working fluids (water and supercritical CO_2), and seven continuous independent parameters of interest (mass flow rate, horizontal extent, vertical drilling depth, rock geothermal gradient, borehole diameter, injection temperature, and rock thermal conductivity) in addition to time. The response measured is the outlet state (outlet pressure and temperature) versus time. The continuous independent variables (plus time) are discretized using equally spaced points as listed in Table 1. This discretization is by no means optimal; however, comparison of interpolated solutions of several randomly chosen design points to simulation runs at the same design points (not shown) suggests this discretization is sufficient to perform accurate multi-dimensional interpolation.

Table 1: Independent variable datasets, [hx] = "utube" or "coaxial", [fluid] = "H2O" or "sCO2"

HDF5 dataset path	Description	Bounds	Units	# of points	Index
/[hx][fluid]/input/mdot	Mass flow rate	[5 to 100]	[kg/s]	26	0
/[hx][fluid]/input/L2	Horizontal extent	[1,000 to 20,000]	[m]	20	1
/[hx][fluid]/input/L1	Vertical drilling depth	[1,000 to 5,000]	[m]	9	2
/[hx][fluid]/input/grad	Rock geothermal gradient	[0.03 to 0.07]	[K/m]	5	3
/[hx][fluid]/input/D	Borehole diameter	[0.2159 to 0.4445]	[m]	3	4
/[hx][fluid]/input/T_i	Injection temperature	[303.15 to 333.15]	[K]	3	5
/[hx][fluid]/input/k_rock	Rock thermal conductivity	[1.5 to 4.5]	[W/m-K]	3	6
/[hx][fluid]/input/time	Simulation output times	[0 to 40]	[years]	161	7

To facilitate tabulating solutions, the Sandia Dakota package (Dalbey et al., 2020) was used to concurrently run over 1,000 simulations at once, with each batch appropriately tiled across the allocated nodes of the job. The results were then parsed and stored into a single HDF5 file. Details of the HDF5 file are presented in Section 3.

3. HDF5 DATASET

The database of numerical solutions is stored in HDF5 file format. HDF5 is a cross-platform binary data format designed to store and perform fast input/output (I/O) operations on large datasets. There are two main object types in an HDF5 file, a dataset (i.e., a multidimensional array of some datatype) and a group. Groups themselves can contain other groups or datasets. The structure of our HDF5 file naturally follows the suite of parametric runs that were performed. At the root HDF5 group, we store two groups that correspond to the heat exchanger type (i.e., "utube", "coaxial"). Each of these groups in turn store four groups, these are the fluid type (i.e., "H2O" or "sCO2"), the fixed parameters group "fixed_params", and the independent variables group "input". The fixed parameters group shown in Table 2 contains scalars that are fixed across the given simulations, whereas the input group shown in Table 1 contains a dataset of a fixed length for each discretized independent variable.

Table 2: Fixed parameters where [hx] = "utube" or "coaxial"

HDF5 dataset path	Description	Value	Units
/[hx]/fixed_params/Pinj	Injection pressure	20.0	[mPa]
/[hx]/fixed_params/Tamb	Ambient temperature	300.0	[K]
/[hx]/fixed_params/Tsurf	Surface temperature, used to set initial temperature distribution	298.15	[K]
/[hx]/fixed_params/pipe_roughness	Pipe roughness used in friction factor calculation	0.025e-3	[m]
/[hx]/fixed_params/rho_rock	Rock density	2750	[kg/m^3]
/[hx]/fixed_params/cp_rock	Rock specific heat capacity	790.0	[J/kg-K]
/coaxial/fixed_params/area_ratio	Ratio of the annular area to pipe area	1.0	N/A
/coaxial/fixed_params/pipe_thickness	Inner pipe wall thickness	0.0192	[m]
/coaxial/fixed_params/pipe_k	Inner pipe wall thermal conductivity (insulated)	0.06	[W/m-K]

The cartesian product of the first six independent datasets corresponds to the simulations that were carried out for the given heat-exchanger / fluid configuration. For simplicity, all four combinations of heat-exchanger / fluid type were evaluated using the same independent variables, resulting in 631,800 simulations per each of the four combinations, totaling to over 2.5 million simulation runs. For each of these runs, we store the outlet states as well as two pre-computed integrated quantities as shown in Table 3.

Table 3: Available output datasets, [hx] = "utube" or "coaxial", [fluid] = "H2O" or "sCO2". Note the left, right singular vectors correspond to a rank k approximation.

HDF5 dataset path	Description
/[hx][fluid]/output/Tout/U	Left singular vectors for outlet temperature state
/[hx][fluid]/output/Tout/sigma	Singular values for outlet temperature state
/[hx][fluid]/output/Tout/Vt	Right singular vectors for outlet temperature state
/[hx][fluid]/output/Pout/U	Left singular vectors for outlet pressure state
/[hx][fluid]/output/Pout/sigma	Singular values for outlet pressure state
/[hx][fluid]/output/Pout/Vt	Right singular vectors for outlet temperature state
/[hx][fluid]/output/We	Available work over forty years, units [GWhr]
/[hx][fluid]/output/Wt	Heat output over forty years, units [GWhr]

As shown for each fluid group, the "output" group contains two datasets labeled "We" and "Wt" and two groups labeled "Tout" and "Pout" that store time-dependent outlet states as a low rank singular value decomposition. The dataset "We" corresponds to the available work (or exergy) integrated over the forty-year operational period and is defined as

$$W_e = \int_0^{T=40} \dot{m}\,(\Delta \mathrm{h} - \mathrm{T}_\infty \Delta \mathrm{s})dt \tag{1}$$

where $\dot{m}$ is the mass flow rate, T_∞ is the ambient temperature, Δs is the change in specific entropy, and Δh is the change in specific enthalpy. This available work is agnostic to the above ground energy conversion configuration and represents the maximum amount of electricity (or useful work) that can be theoretically extracted based on the second law of thermodynamics. Actual electricity generation

is addressed later and depends on the energy conversion system employed and is significantly less than the theoretical maximum for temperatures encountered in geothermal systems.

The dataset W_t is the heat (thermal energy) output over the forty-year operation period and is defined as

$$W_t = \int_0^{T=40} \dot{m}\,\Delta h dt \tag{2}$$

The dimensionality of these two datasets corresponds to the first six independent variables and can be indexed accordingly.

As mentioned earlier, for the time-dependent datasets, instead of directly storing the outlet state which would require (161 × 631,800) floats of storage per outlet state, we instead perform a singular value decomposition and store a low rank approximation for each outlet state. That is, we only store the rank k left singular vectors U, singular values σ, and right singular vectors V^T as shown in Table 3.

To obtain these values, the raw outlet time-dependent data is reshaped from L0×L1×L2×L3×L4×L5×L6×L7 into an m × n matrix M, where m = L7, the number of equally spaced simulation output times, and where n = 631,800 = L0×L1×L2×L3×L4×L5×L6, total number of simulations for a given heat exchanger / working fluid combination. The lengths are given by column 5 of Table 1. The singular value decomposition is then performed on the matrix M, compressing the outlet state storage to k + k*(161 + 631800) floats, where k corresponds to the number of singular values that were kept. The rank k outlet states approximation M_k (e.g., all temperature states or all pressure states for given heat exchanger/fluid configuration) can then be recovered as

$$M_k = \sum_{i=1}^{i=k} \sigma_i U_i V_i^T \tag{3}$$

This rank k singular value decomposition gives the best rank k approximation to the original matrix M. The rank k matrix approximation M_k can then be reshaped back into the original L0×L1×L2×L3×L4×L5×L6×L7 multi-dimensional array which can be more readily used for interpolation, querying, plotting, etc.

Storing the singular vectors and values for a rank 4 approximation for the u-tube dataset gives a 40x compression ratio and is sufficient to approximate the original data to within a relative tolerance of 0.0017 (or 0.17%) across any of the outlet states at any point in time. Similarly, the coaxial dataset achieves 40-55x compression ratios with a relative tolerance of 0.005 (or 0.5%). As shown in Figure 3, this low rank approximation is possible because the singular values quickly drop off. To further reduce the size of the data, we find storing the singular vectors and values in 32-bit precision is acceptable. In this manner, the HDF5 dataset is reduced to only 70 MB.

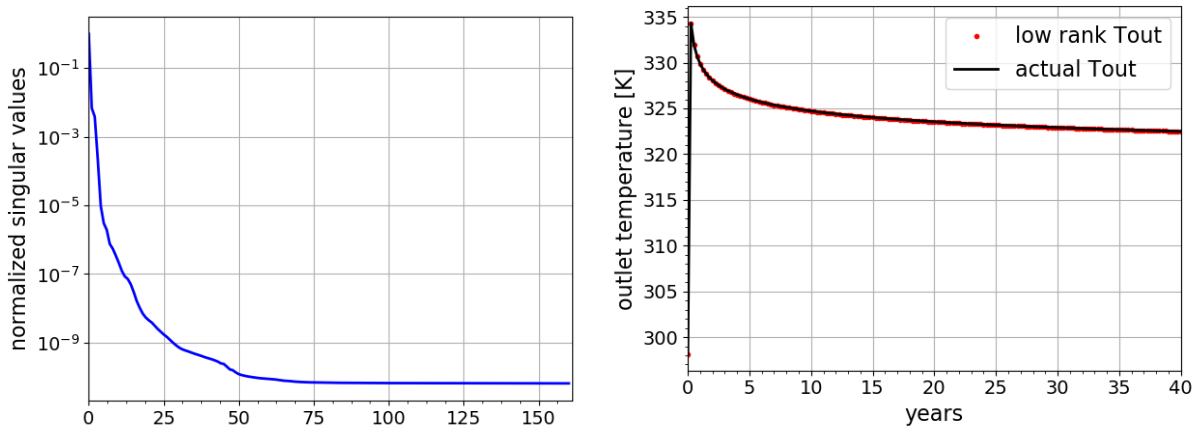

Figure 3: (Left) Normalized singular values for sCO_2 outlet temperature dataset for the u-tube. Similar decay of singular values was observed for the outlet pressure as well as for other heat exchanger / working fluids combinations. (Right) Example comparison of outlet temperature at a given query point compared to the rank 4 approximation.

3.1 Python scripts

In the accompanying Python scripts, we provide an input class that wraps the HDF5 dataset and unpacks the data. It can be instantiated for each of the four heat-exchanger / working fluid combinations. The constructor takes three arguments: (1) the HDF5 closed-loop geothermal system database file; (2) the heat-exchanger type (i.e., "u-tube", "coaxial"); and (3) the fluid type (i.e., "H2O", "sCO2"). In turn, the object will contain multi-dimensional NumPy arrays "We", "Wt", "Tout", and "Pout", corresponding to the available work, heat output, and temperature and pressure output, respectively. As can be deduced from Table 1, "We", and "Wt" have shape L0xL1xL2xL3xL4xL5xL6 and are time-independent, whereas "Tout" and "Pout" have shape L0xL1xL2xL3xL4xL5xL6xL7, where the right most index corresponds to time. In addition to these member variables, the Python class has several member functions that can be

used to 1) interpolate the outlet temperature and pressure at a specified design point, 2) interpolate the average heat output and average available work over the forty-year operational period at a user specified point, and 3) interpolate the power output and heat output as a function of time at a user specified point.

The accompanying Jupyter notebook contains several examples illustrating these cases. Jupyter notebook example outputs for the u-tube are shown below in Figure 4 through Figure 7.

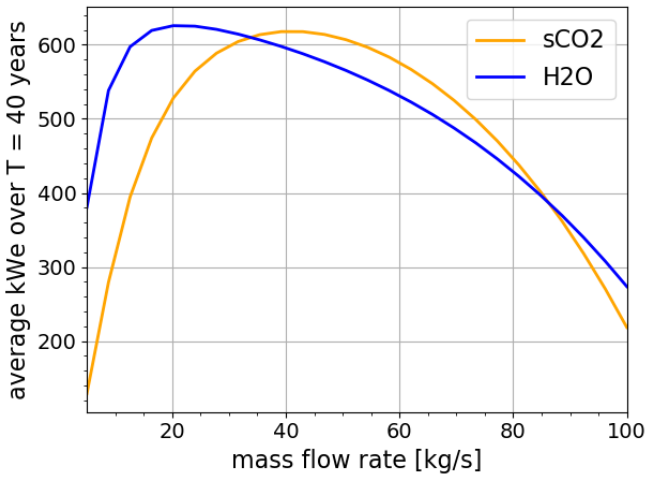

Figure 4: Example 1. Comparison of the average available power for both sCO_2 and H_2O over T = 40 years at a known point in the design space (i.e., no interpolation needed). Results are evaluated at a horizontal length = 9,000 m, vertical depth = 3,000 m, thermal gradient = 60 K/km, borehole diameter = 0.2159 m, injection temperature = 333.15 K, and rock thermal conductivity = 3.0 W/m-K. Corresponding bottom-hole temperature is 205°C (478 K).

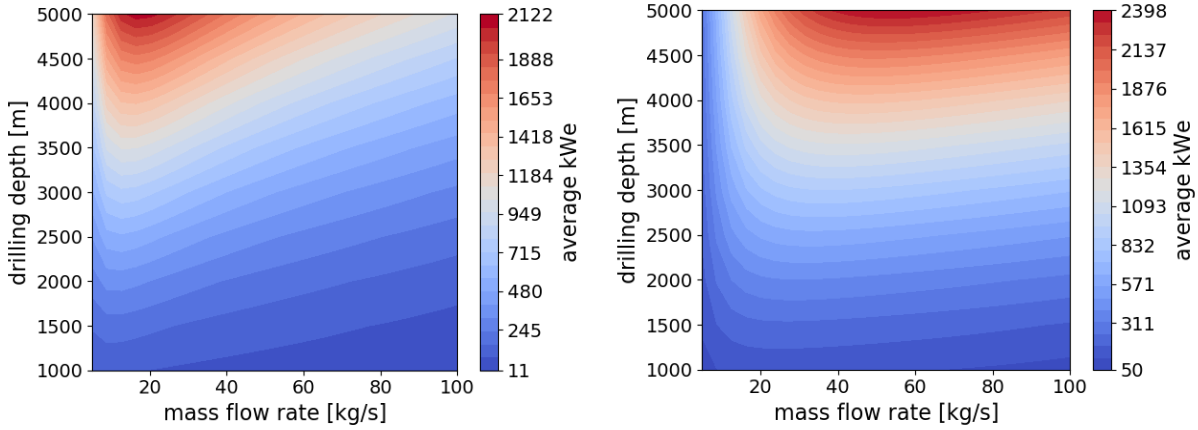

Figure 5: Example 2. Average available power for the u-tube heat exchanger over T = 40 years as a function of the mass flow rate and drilling depth. H_2O working fluid (left) and sCO_2 working fluid (right). Results are evaluated at a horizontal length of 9,000 m, thermal gradient of 70 K/km, borehole diameter equal to 0.3302 m, injection temperature equal to 303.15 K, and rock thermal conductivity equal to 3.0 W/m-K. Corresponding bottom-hole temperature ranges from 95°C to 375°C (368 to 648 K).

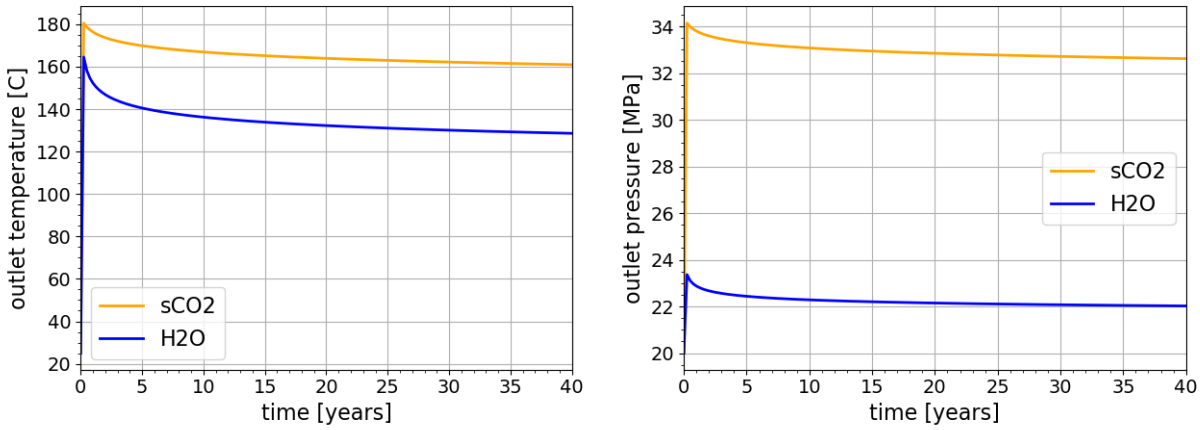

Figure 6: Example 3. Multi-dimensional interpolation of the outlet temperature and pressure as a function of time for the u-tube heat exchanger at a user specified point that does not correspond to a simulation run (i.e., an off-grid point). Here, the design point is mass flow rate = 25.1 kg/s, horizontal extent = 15,140 m, vertical depth = 4,100 m, thermal gradient = 65 K/km, borehole diameter = 0.3 m, injection temperature = 315 K, and rock thermal conductivity = 2.5 W/m-K. Corresponding bottom-hole temperature is 291.5°C (565 K).

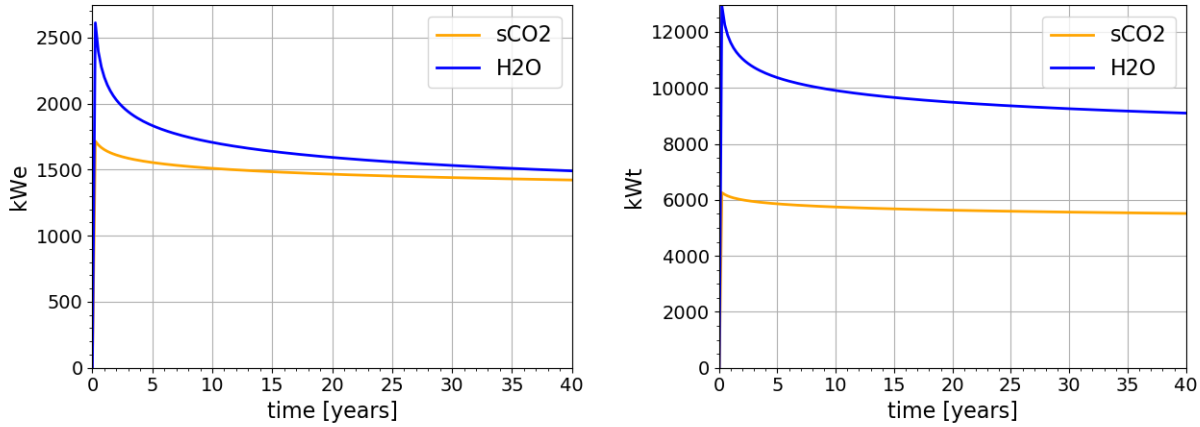

Figure 7: Example 4. Multi-dimensional interpolation of the available power and heat as a function of time for the u-tube heat exchanger at a user specified point that does not correspond to a simulation run (i.e., an off-grid point). Here, the design point is mass flow rate = 25.1 kg/s, horizontal extent = 15,140 m, vertical depth = 4,100 m, thermal gradient = 65 K/km, borehole diameter = 0.3 m, injection temperature = 315 K, and rock thermal conductivity = 2.5 W/m-K. Corresponding bottom-hole temperature is 291.5°C (565 K).

3.2 Dataset limitations

Before proceeding to Section 4, several clarifying comments need to be made regarding the datasets. First, not all design points will result in viable solutions; that is, some design points lose heat to the formation. Similarly, other designs gain heat from the formation but will result in no available work that can be extracted, see Figure 8. No attempt is made to prune these solutions from the database.

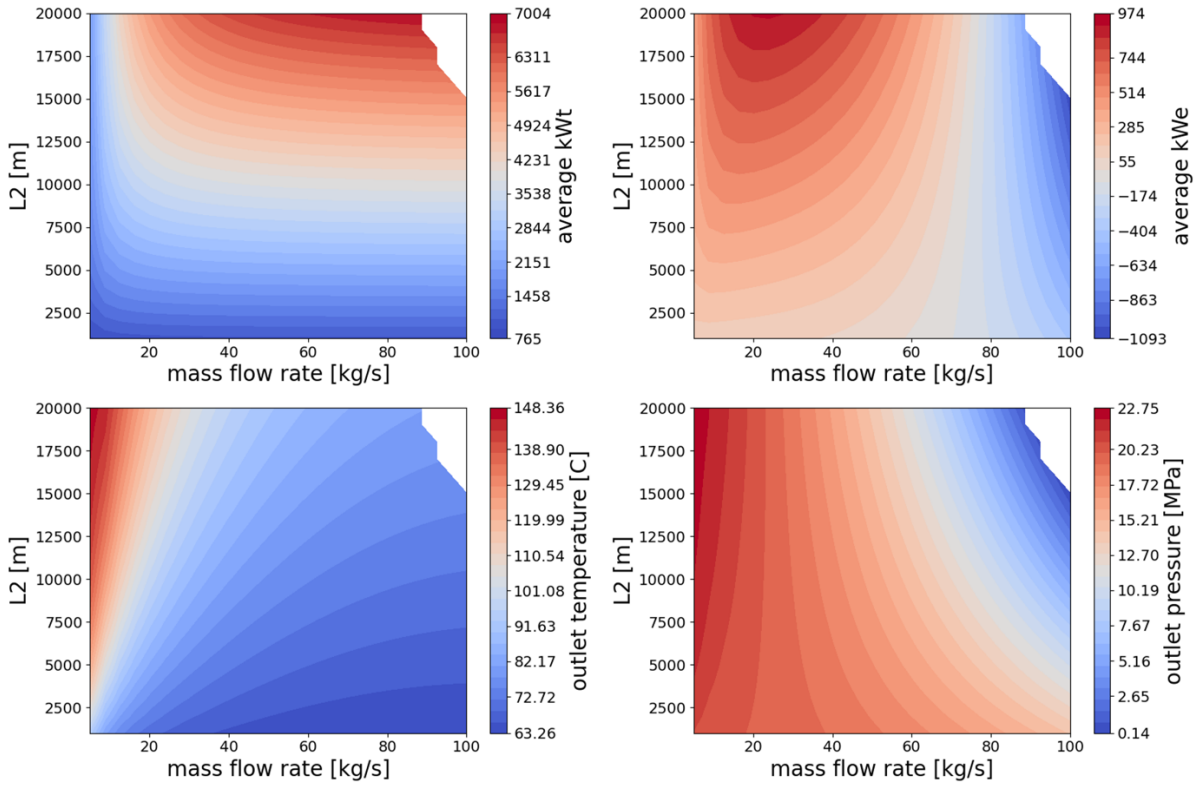

Figure 8: H_2O results for the coaxial heat exchanger (flow down the annulus) at the design point specified by vertical depth = 4,500 m, thermal gradient = 50 K/km, borehole diameter = 0.3302 m, injection temperature = 333.15 K, and rock thermal conductivity = 1.5 W/m-K. Corresponding bottom-hole temperature is 250°C (523 K). Here, the outlet temperature and pressure correspond to end of life. Design points that would flash have been pruned (white area) from the dataset. These solutions could be obtained by increasing the injection pressure.

Second, all datasets are at a single injection pressure of 20 MPa. Consequently, the coaxial dataset required pruning some solutions due to too large of pressure drops for the specified injection pressure. These solutions are marked with "not a number," i.e., NaNs. These large pressure drops occur for both sCO_2 and water due to the smaller hydraulic diameters present in the coaxial system. An example of these large pressure drops is shown in Figure 8 along with other solution contours for reference. For the coaxial water results, about 22.5% of the design points were pruned based on the saturation pressure cutoff. For coaxial sCO_2 results, about 27% of the design points were pruned based on a pressure cutoff designed to give a 1 MPa buffer with respect to the critical point. In both cases, the pressure cutoff was implemented through a change of variables in the material property tables. In both cases, the pressure cutoff was implemented through a change of variables in the material property tables. In the case of the sCO_2 tables, this change of variables results in a 1 MPa buffer with respect to the saturation curve and a 1 MPa buffer above the critical pressure when the temperature is above the critical value. Simulation runs referencing a pressure outside the table limits were pruned. Lastly, no pruning was needed for the u-tube results, as the maximum pressure drop across all u-tube simulation runs was less than 7 MPa.

4. TECHNO-ECONOMIC ANALYSIS (TEA)

A script was developed that combines the subsurface simulation results (Section 3) with power plant models and cost correlations to estimate electricity generation output and overall levelized cost of electricity (LCOE) and heat (LCOH). For water as the heat transfer fluid, an organic Rankine cycle was assumed with efficiency correlations for conversion from heat to electricity based on the thermal efficiency correlations developed by Augustine (2009) and utilization efficiency correlations (based on produced exergy) developed by Beckers (2016) and implemented in GEOPHIRES (Beckers and McCabe, 2019). For sCO_2 as the circulating fluid, we assumed a direct turbine expansion cycle where the circulating CO_2 is also the working fluid through the cycle. We implemented the approach by Wang et al. (2022), where, after turbine expansion, the CO_2 gets cooled ("pre-cooling"), followed by compression and then cooling again ("post-cooling") to injection conditions. CO_2 temperature and pressure at each step throughout the cycle are either calculated or user-specified. CoolProp tables are used for obtaining values for properties such as enthalpy and entropy. Turbine power generation and compressor power consumption are based on a user-provided isentropic efficiency. Pre-cooling and post-cooling assume direct air cooling with fans. Fan power consumption is calculated based on required air flow rate and assuming 0.25 kWe per kg/s of required air (Augustine, 2009).

Simple cost correlations are implemented to calculate capital, and operation and maintenance (O&M) costs. Drilling costs and surface plant costs are considered to estimate overall system capital cost. Drilling costs are calculated by multiplying total drilling depth with a drilling cost per m, with $1,000/m as default value. Existing well drilling cost correlations (e.g., Lowry et al., 2017) are not implemented

because closed-loop well design may be different (e.g., long open-hole laterals) and total well drilling measured depth may be beyond typical drilling depths (Beckers and Johnston, 2022). Surface plant costs are based on the size of the plant, with plant-specific cost values based on findings by Beckers and Johnston (2022), Beckers et al. (2022), and Beckers and McCabe (2019). For electricity generation, a default value of \$3,000/kW_e is assumed. For direct-use heat, the surface plant cost assumes a default value of \$100/kW_{th}. This cost represents costs for the heat exchanger, piping, and valves but not a district heating system. The O&M cost is calculated as a percentage of the surface plant investment cost with 1.5% as default value, based on research by Beckers and Johnston (2022). Because the fluid circulates in a closed-loop, no scaling or corrosion issues are anticipated and no wellfield maintenance costs are considered. For direct-use, pumping costs are accounted for by considering a user-provided electricity rate. For electricity as end-use, the pumping power is subtracted from the plant electricity output. Capital or O&M costs for potential exploration, well redrilling, well field maintenance, and land leasing are not considered. The levelized cost for either electricity or heat is calculated assuming a simple discounting model with a user-specified discount rate, similar to the "standard discounting model" in GEOPHIRES (Beckers and McCabe, 2019).

The script is developed as a Python class where a TEA object is created with user-specified conditions (flow rate, depth, fluid type, etc.). The class has different functions to calculate production temperature and pressure, thermal output and electricity generation, and capital, O&M, and levelized costs. The class also has a function to verify the user input to ensure each parameter value falls within the allowable range. The script prints results to the screen, including average production temperature, pressure, thermal output, and electricity generated, and capital cost breakdown, O&M cost, and levelized cost. In addition, several plots are created to show production temperature, pressure, thermal output, and electricity production over the plant lifetime as well as heat and electricity generated each year.

To demonstrate the TEA script, Example 1 is revisited to calculate thermal output and net electricity generation as well as capital, O&M, and levelized costs for both water and sCO_2 as heat transfer fluid. This example assumes a U-loop configuration with a depth of 3,000 m, horizontal length of 9,000 m (1 lateral), geothermal gradient of 60°C/km, borehole diameter of 0.2159 m, injection temperature of 60°C, rock thermal conductivity of 3 W/m-K, and system lifetime of 40 years. The corresponding bottom-hole temperature is 205°C. The flow rate for water is set to 20 kg/s and for sCO_2 to 40 kg/s. Default values are assumed for discount rate, plant specific cost, drilling cost, and plant O&M cost. Fixed parameters (e.g., injection pressure of 200 bar) are provided in Table 2. All assumptions are listed in Table 4. Simulation results for water as the heat transfer fluid are provided in Table 5 and Figure 9. Simulation results for sCO_2 as the heat transfer/working fluid are provided in Table 5 and Figure 10. Using water, average heat production is about 3.9 MW_{th} and average electricity generation about 285 kW_e. In comparison with the results for Example 1 in Figure 4, the net electricity (285 kW_e) is about 50% of the exergy or available power (i.e., operating at Carnot efficiency) at 20 kg/s (about 600 kW_e), a result of the inherent cycle inefficiencies when a fluid undergoes compression, expansion, and heat exchange. The LCOH is estimated at \$39/MWh and the LCOE at \$426/MWh. Using sCO_2, the average heat production is about 3.1 MW_{th} and the average electricity generation is 289 kWe. The corresponding LCOH is \$39/MWh and the LCOE is \$426/MWh. The O&M cost in each configuration is only a few thousand to tens of thousands of dollars, much lower than typical O&M cost for a geothermal plant. This is a direct result of assuming no maintenance cost is required for the wellfield, and the plant equipment for heating or electricity units are "off the shelf" technology not requiring constant supervision. Results are not optimized because potentially higher thermal output or electricity generation can be obtained for different flow rate, turbine outlet pressure, and pre-cooling temperature decrease. Given that a run is performed in a fraction of a second, the user can quickly explore performance under various conditions to find an optimum.

Table 4: TEA example input conditions based on Example 1 shown in Figure 4.

Parameter	Value
Configuration	U-loop with 1 lateral
Heat transfer fluid	Water and sCO_2
End use	Heating and electricity
Flow rate	20 kg/s for water / 40 kg/s for sCO_2
Vertical depth	3,000 m
Horizontal length	9,000 m
Geothermal gradient	60°C/km (bottom-hole temperature of 205°C)
Borehole diameter	0.2159 m
Injection temperature	60°C
Injection pressure (fixed parameter)	200 bar
Rock thermal conductivity	3 W/m-K
Rock specific heat capacity (fixed parameter)	790 J/kg-K
Rock density (fixed parameter)	2,750 kg/m^3
System lifetime	40 years
Drilling cost per meter	\$1,000/m
O&M cost plant as percentage of plant capital cost	1.5%
Discount rate	7%
Direct-use heat plant cost	\$100/kW_{th}
Power plant cost (for electricity generation)	\$3,000/kW_e

Dead-state temperature	20°C
Dead-state pressure	1 bar
Turbine isentropic efficiency (for sCO_2 electricity)	90%
Generator efficiency (for sCO_2 electricity)	98%
Compressor isentropic efficiency (for sCO_2 electricity)	90%
Turbine outlet pressure (for sCO_2 electricity)	79 bar
Pre-cooling temperature decline (for sCO_2 electricity)	5°C

Table 5: TEA example simulation results.

Parameter	Value	
Water as heat transfer fluid (20 kg/s)		
	Direct-Use Heating	Electricity
Average production temperature	107°C	
Average production pressure	207 bar	
Average heat production	3.9 MW_{th}	
Average electricity production	N/A	285 kW_e
Total capital cost	$15.5M	$16.2M
Drilling cost	$15M	
Plant cost	$0.5M	$1.2M
Total O&M cost	$8k/year	$19k/year
Levelized cost	LCOH = $31/MWh	LCOE = $438/MWh
sCO_2 as heat transfer/working fluid (40 kg/s)		
	Direct-Use Heating	Electricity
Average production temperature	96°C	
Average production pressure	234 bar	
Average heat production	3.1 MW_{th}	
Average electricity production	N/A	289 kW_e
Total capital cost	$15.4M	$16.4M
Drilling cost	$15M	
Plant cost	$0.4M	$1.4M
Total O&M cost	$6k/year	$22k/year
Levelized cost	LCOH = $39/MWh	LCOE = $426/MWh

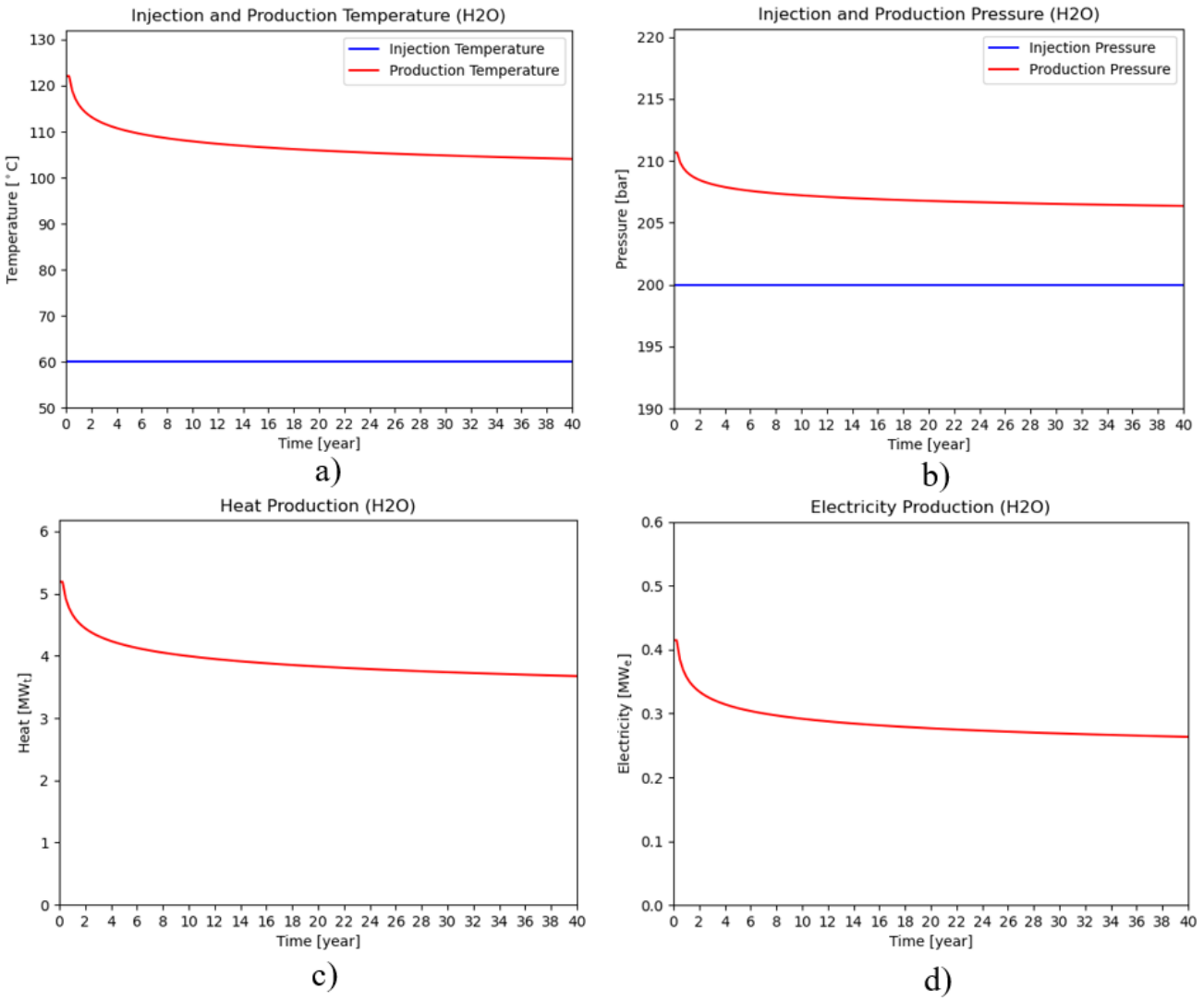

Figure 9: Production temperature, pressure, heat, and electricity for U-loop configuration defined in Table 4 with water as heat transfer fluid.

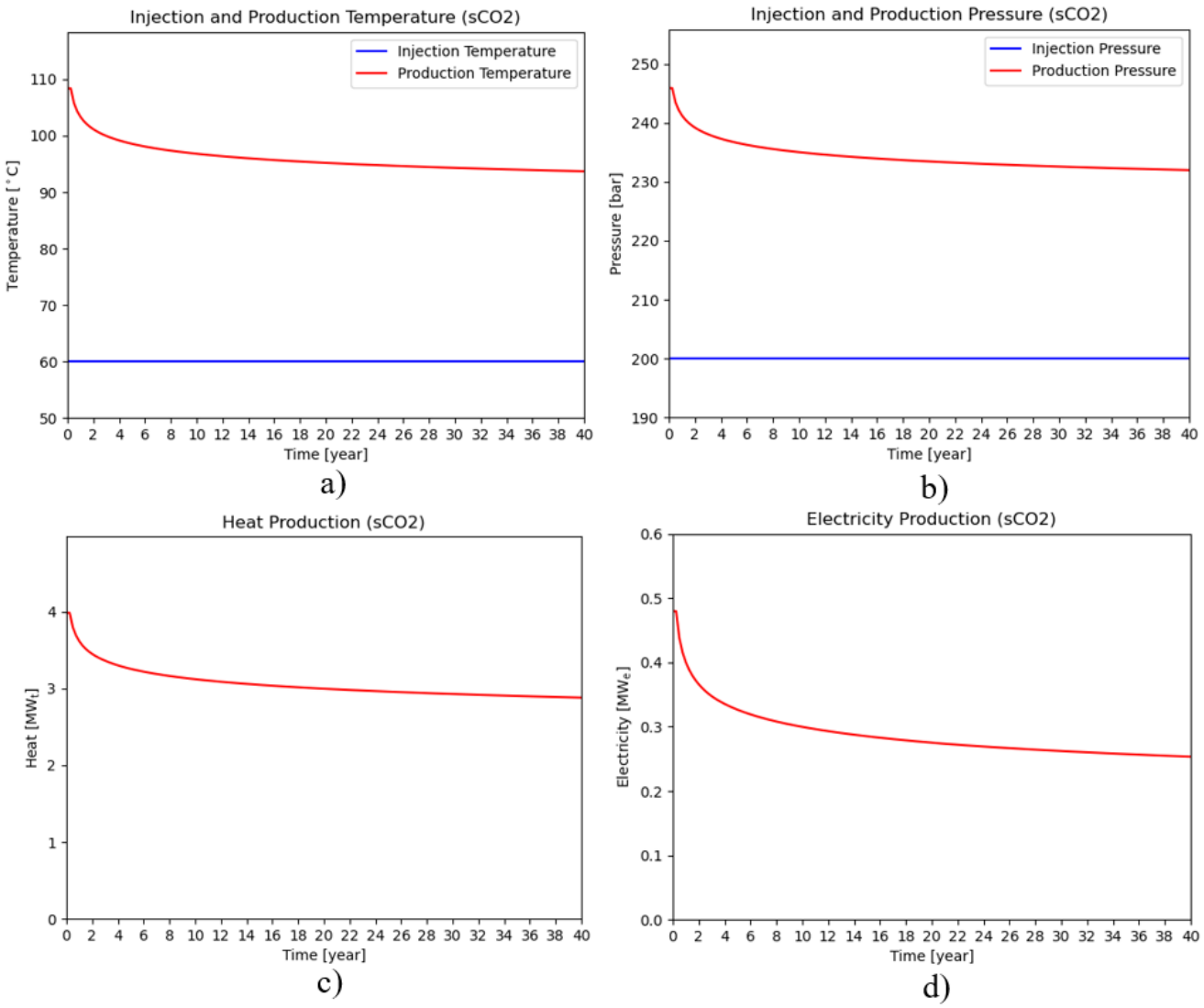

Figure 10: Production temperature, pressure, heat, and electricity for U-loop configuration defined in Table 4 with sCO_2 as heat transfer/working fluid.

5. CONCLUSIONS

A consortium of U.S. national laboratories and universities, funded by the U.S. Department of Energy Geothermal Technologies Office, is studying technical performance and cost-competitiveness of closed-loop geothermal systems. Various tasks are undertaken by the different consortium partners including closed-loop geothermal simulation tool development and assessing performance of various designs under different operating conditions. Several publications have documented the results of our study so far. This paper presents results of numerical simulations using Sandia's Sierra software suite to estimate heat extraction for various conditions, and development of a TEA tool based on NREL's GEOPHIRES framework to assess capital, O&M, and levelized costs.

Millions of subsurface simulations were run to pre-calculate and store (in HDF5 format) production temperatures and pressures for a wide range of closed-loop system scenarios and conditions. We considered both a U-loop and co-axial design, water and sCO_2 as heat transfer fluid, and a range in wellbore depth, wellbore horizontal length, injection temperature, flow rate, geothermal gradient, wellbore diameter, and rock thermal conductivity. The subsurface results are imported by a TEA script developed in Jupyter Notebook for post-processing to estimate thermal or electricity output and calculate capital, O&M, and levelized cost of energy (heat or electricity). A standard discounting model is considered to discount future revenue and expenses to today's value. The Python scripts and dataset have been uploaded online and can run in the cloud to allow the user to apply the tool without requiring downloading the dataset and scripts or installing any software. The Jupyter Notebook includes a widget-based interface to allow users without coding experience to run the tool.

ACKNOWLEDGMENTS

This work was authored in part by the National Renewable Energy Laboratory, operated by Alliance for Sustainable Energy, LLC, for the U.S. Department of Energy (DOE) under Contract No. DE-AC36-08GO28308, and Sandia National Laboratories, managed and operated by NTESS under DOE NNSA contract DE-NA0003525. Funding provided by the U.S. Department of Energy Office of Energy Efficiency and Renewable Energy Geothermal Technologies Office. The views expressed herein do not necessarily represent the views of the DOE or the U.S. Government. The U.S. Government retains and the publisher, by accepting the article for publication, acknowledges that the U.S. Government retains a nonexclusive, paid-up, irrevocable, worldwide license to publish or reproduce the published form of this work, or allow others to do so, for U.S. Government purposes.

REFERENCES

Augustine, C. R.: Hydrothermal spallation drilling and advanced energy conversion technologies for engineered geothermal systems, (2009), Doctoral dissertation, Massachusetts Institute of Technology.

Beckers, K. J. H. F. Low-temperature geothermal energy: systems modeling, reservoir simulation, and economic analysis (2016), Doctoral Dissertation, Cornell University.

Beckers, K. F., and Johnson, H. E.: Techno-economic performance of Eavor-Loop 2.0. In Proceedings, 47th workshop on geothermal reservoir engineering, Stanford, California (2022).

Beckers, K. F., and McCabe, K.: GEOPHIRES v2.0: Updated geothermal techno-economic simulation tool, (2019), Geothermal Energy, 7(1), 1-28.

Beckers, K. F., Rangel-Jurado, N., Chandrasekar, H., Hawkins, A. J., Fulton, P. M., & Tester, J. W.: Techno-economic performance of closed-loop geothermal systems for heat production and electricity generation. Geothermics, 100, (2022), 102318.

Bell, I. H., Wronski, J., Quoilin, S., & Lemort, V. (2014). Pure and Pseudo-pure Fluid Thermophysical Property Evaluation and the Open-Source Thermophysical Property Library CoolProp. *Industrial & Engineering Chemistry Research*, *53*(6), 2498-2508. https://doi.org/10.1021/ie4033999

Dalbey, K., Eldred, M. S., Geraci, G., Jakeman, J. D., Maupin, K. A., Monschke, J. A., Seidl, D. T., Swiler, L. P., Tran, A., & Menhorn, F. (2020). Dakota A Multilevel Parallel Object-Oriented Framework for Design Optimization Parameter Estimation Uncertainty Quantification and Sensitivity Analysis: Version 6.12 Theory Manual. *SAND2020-4987, Sandia National Laboratory*.

DOE - U.S. Department of Energy. (2022). "Enhanced Geothermal Systems". https://www.energy.gov/eere/geothermal/enhanced-geothermal-systems.

Horne, R.: Geothermal Closed-Loop Simulator" (2022), available at https://pangea.stanford.edu/ERE/db/Roland/ClosedLoop/.

Lowry, T., Finger, J., Carrigan, C., Foris, A., Kennedy, M., Corbet, T., Doughty, C., Pye, S., Sonnenthal, E.: GeoVision Analysis Supporting Task Force Report: Reservoir Maintenance and Development Sandia National Laboratories, Albuquerque, NM (2017), SAND2017-9977.

Malek, A.E., Adams, B., Rossi, E., Schiegg, H.O., Saar, M.O., 2021. Electric Power Generation, Specific Capital Cost, and Specific Power for Advanced Geothermal Systems (AGS). 46th Workshop on Geothermal Reservoir Engineering. Stanford University, Stanford, California. February 15-17, 2021.

Morita, K., Bollmeier, W. S., & Mizogami, H. (1992a). Analysis of the Results from the Downhole Coaxial Heat-Exchanger (Dche) Experiment in Hawaii. 20th Anniversary - Geothermal Resources Council, 16, 17-23.

Morita, K., Bollmeier, W. S., & Mizogami, H. (1992b). An Experiment to Prove the Concept of the Downhole Coaxial Heat-Exchanger (Dche) in Hawaii. 20th Anniversary - Geothermal Resources Council, 16, 9-16.

Oldenburg, C., Pan, L., Muir, M., Eastman, A., Higgins, B.S. (2016). Numerical simulation of critical factors controlling heat extraction from geothermal systems using a closed loop heat exchange method. In: Proceedings, 41st Workshop on Geothermal Reservoir Engineering, Stanford, California, February 22-24, 2016.

Ramey, H. Jr.: Wellbore heat transmission, Journal of Petroleum Technology 14.04 (1962): 427-435.

Sierra Thermal Fluids Development Team. (2021). *SIERRA Multimechanics Module: Aria User Manual - Version 5.0* (SAND2021-3921). https://www.osti.gov/biblio/1777075.

SimTech: IPSEpro 8.0, SimTech Simulation Technology, Graz, Austria (2021).

Vasyliv, Y., Bran-Anleu A., G., Kucala, A., Subia, S., & Martinez, M. (2021). Analysis and Optimization of a Closed Loop Geothermal System in Hot Rock Reservoirs. Geothermal Resources Council Transactions, 45.

Wang, X., Pan, C., Romero, C. E., Qiao, Z., Banerjee, A., Rubio-Maya, C., and Pan, L.: Thermo-economic analysis of a direct supercritical CO2 electric power generation system using geothermal heat. Frontiers in Energy, 16(2), (2022), 246-262.

White, M., Martinez, M., Vasyliv, Y., Bran-Anleu A., G., Parisi, C., Balestra, P., Horne, R., Augustine, C., Pauley, L., Hollett, D., Bettin, G., Marshall, T., & Group, C. L. G. W. (2021). Thermal and Mechanical Energy Performance Analysis of Closed-loop Systems in Hot-Dry-Rock and Hot-Wet-Rock Reservoirs. *Geothermal Resources Council Transactions*, *45*.